

CHAPTER 8

POLYTYPIISM IN TaS_2 CRYSTALS

	CONTENTS	PAGES
8.1	Introduction	147
8.2	Experimental	149
8.3	Identification of Polytypes	150
8.4	Results and Discussion	153
8.5	Conclusions	159
8.6	References	160
	Captions of the figures	162
	Figures	163

8.1 Introduction

In recent years the phenomenon of polytypism has gained much importance in layered structure crystals. A substance is said to be polymorphous when it can exist in two or more forms with different crystal structures, whereas the polytypism, can be justifiably regarded as a special case of polymorphism and called "one dimensional" polymorphism. Hence a solid can be crystallized into more than one modification without changing its chemical composition but which differs in number and manner of stacking of layers in the unit cell. A decade ago the detailed studies of "polymorphism and polytypism in crystals" have been published by

Verma and Krishna¹⁾. Recently, a review on "polytypism and stacking faults in crystals with layer structure" has been published by Trigunayat and Verma.²⁾

The various polytypes of the same polytypic material have been found to have different physical properties which lead to a considerable solid state interest. Polytypism is mainly observed in layered crystals, belonging to the groups V and VI. The various polytypic modifications are assembled in three groups, viz.

- (i) these having a prismatic surrounding of the metal by the chalcogen atoms,
- (ii) these having an octahedral surrounding and
- (iii) these having alternating layers with prismatic and octahedral surrounding.

1T-TaS_2 belongs to a octahedral surrounding of the metal by the chalcogen atoms and has CdI_2 type structure.

Several extensive theoretical and experimental investigations in the search of possible polytypes of TaS_2 have been carried out and systematic investigations of the Ta-S system have been reported by Biltz and Kecher³⁾, by Hagg and Schonberg⁴⁾ and by Jellinek⁵⁾ and various Ta_xS_y compounds have been found in these studies.

In view of the almost complete disagreement of the results presented in ⁴⁾ and ³⁾ Jellinek reinvestigated the Ta-S system, mainly by X-ray powder method ⁵⁾ and observed the following polytypes.

1T-TaS₂, 2H-TaS₂, 3R-TaS₂ and 6R-TaS₂ indicating that the repeat units in the c-direction have a thickness of one, two, three and six TaS₂ slabs respectively. Further investigations have recently revealed the existence of 4H(b) - form ⁶⁾ and a superstructure of 1T-TaS₂ ⁷⁾. The polytypes of TaS₂ have various designations : 1T-AbC, 2H, AbA - CbC, 3R, AbA-BoB-CaC, 4Hb, AbA-CbA-CbC-AbC where the stacking sequence is given for a unit cell.

Number of the workers have carried out the work on the polytypic study of TaS₂ but they have used the single crystals which were incorporated with some transporting agents.

In this chapter the results of a study of polytypism in TaS₂ single crystals grown by direct vapour transport method are presented and discussed. Density of dislocations determined is also reported.

8.2 Experimental

The as-grown 2 to 5 mm wide and 200 to

700 μm thick TaS_2 crystals were selected for X-ray oscillation studies. The c-axis oscillation photographs of the crystals are not suitable for the identification of polytypes as they generally show streaking and smearing of diffraction spots. However, the c-dimension can also be evaluated from a-axis oscillation photographs⁸⁾, which are relatively free from these unwanted features. Therefore, a-axis oscillation photographs were used for the identification of polytypes. The crystals were mounted along the a-axis, an oscillation range of 15° was selected in such a way that it varied between 25° and 40° between the directions of the incident X-ray beam and the c-axis. This range was particularly chosen to record a large number of (01.l) reflections where l index increased from the centre of the film towards its end. Such X-ray photographs of all the crystals were taken with a cylindrical camera of radius 3.0 cm and a collimator of aperture 0.101 cm. The size of the focal spot was 1 mm^2 ; $\text{CuK}\alpha$ radiation (wavelength 1.5418 \AA) was used.

8.3 Identification of Polytypes

When a-axis is vertical and taken as the axis of oscillation, the reciprocal lattice nets c^*b^* are horizontal. The zero layer b^*c^* net is shown in Fig. 8.1. Since the 'a' dimension ($= b$) which is equal

for all polytypes, has a small value (3.426 \AA), the lines parallel to c^* on the reciprocal lattice nets are widely spreaded. Hence the range of oscillation could be so chosen upon a net that the number of consecutive lattice points corresponding to a fixed value of b^* (and successive value of c^*) come to produce diffraction spots on one side of the X-ray film in the limited oscillation range of 15° . In this way a large number of spots could be obtained whose indices were uniquely defined. Considering Fig. 8.1 if ζ_1 denotes the ζ value of the n th diffraction spot (measured from Bernal chart) and ζ_2 denotes the ζ value of the $(n + q)^{\text{th}}$ spot, in a series of consecutive spots corresponding to a fixed value of b^* , say $2b^*$, we have

$$\zeta_1^2 = (2b^*)^2 + (nc^*)^2 \quad \dots \quad (8.1)$$

$$\zeta_2^2 = (2b^*)^2 + \{(n + q)c^*\}^2 \quad \dots \quad (8.2)$$

Due to the restricted oscillation (15°) and on account of the wide spacing of constant b^* lines, no confusion like the duplication of co-ordinates corresponding to a single ζ -value could arise. In fact, by a suitable choice of the range of oscillation upon the zero level reciprocal lattice net, the series

of (10.0) to (10.2n) consecutive (10.1) spots, which have been used by Mitchell⁹⁾ for the determination of the stacking sequence of the various polytypes, could be obtained. The above expressions apply to both hexagonal and rhombohedral polytypes, namely, $-h + k + l = 3n$ has to be taken into account while estimating n and $(n + q)$.

Expressions (8.1) and (8.2) were derived taking into account the zero layer on the zero level of the reciprocal lattice. The origin of lattice points, measured from the origin of the reciprocal lattice, are the same as their corresponding ξ -values, which are measured from the axis of rotation. However, for the first layer the origin of the reciprocal lattice is shifted from the axis of rotation by an amount $a^* \sin 30^\circ$, if a -axis is the axis of rotation of the crystal. Therefore, the first layer line of the reciprocal lattice distance (say, S) of a lattice point from the origin is not the same as its ξ -value. For (01.1), 1-spots which lie on the c^* axis, the S -values are related to ξ -values as

$$S_1^2 = (\xi_1)^2 - (a^* \sin 30^\circ)^2$$

and

$$S_2^2 = (\xi_2)^2 - (a^* \sin 30^\circ)^2$$

where

$$S_1 = nc^* \text{ and}$$

$$S_2 = (n + q)c^*$$

8.4 Results and Discussion

A 15° a -axis oscillation photograph of $1T-TaS_2$ crystal is shown in Fig. 8.2, taken in the oscillation range ($25 - 40^\circ$). The value of C parameter was evaluated from this figure, following the procedure outlined in section 8.3. Taking the first layer the following measurements were made

$$\begin{aligned} \zeta_1 & \text{ for } n\text{th spot} = 0.5575 \\ \zeta_2 & \text{ for } (n + 3)\text{th spot} = 1.33 \\ \text{Now } S_1^2 & = \zeta_1^2 - (a^* \sin 30) ^2 \\ S_1^2 & = (0.5575)^2 - 0.06749 \\ S_1^2 & = 0.24332 \\ S_1 & = 0.49338 \\ S_2^2 & = (1.3)^2 - 0.06749 \\ S_2^2 & = 1.69 - 0.06749 \\ S_2^2 & = 1.62251 \end{aligned}$$

$$S_2 = 1.27377$$

Since the 01.1 spots lie on c^* axis we have

$$S_1 = nc^*$$

$$S_2 = (n + 3)c^*$$

$$\therefore S_2 - S_1 = 3c^*$$

$$\therefore 1.27377 = 0.49338 = 3c^*$$

$$\therefore c^* = 0.26013$$

$$\text{Now } c = \frac{\lambda}{c^*}$$

$$= \frac{1.5418}{0.26013}$$

$$= 5.9270 \text{ \AA (neglecting shrinkage error)}$$

The value of 'a' as determined from the spacing between the layer lines comes out to be 3.426 \AA.

$$\text{Since } nc^* = S_1$$

$$n = S_1/c^*$$

$$= 2.$$

Therefore the diffraction corresponding to ξ_1 has

indices 01.2.

It can be noticed that the spots on the *a*-axis oscillation photograph show mirror symmetry, about the zero layer line. This is due to an actual mirror plane perpendicular to 'a' in the structure. These values of 'a' and 'c' are in agreement with the reported ASTM data values for 1T-TaS₂.

The phase transformation in layered crystals is a common phenomenon¹⁾. Generally the higher polytypes of a crystal transform into a lower common polytype and vice versa by heating the crystal nearly to its melting point. This phenomenon has been observed in CdI₂ and PbI₂ crystals (10, 11). A few experiments were also conducted in the present investigation with a view to observe phase transformation in 1T-TaS₂ crystals.

A crystal having a 1T-TaS₂ type structure at room temperature was heated to 600°C in atmosphere for 60 min. and the oscillation photograph was taken as shown in Fig. 8.3. This photograph shows the appearance of a number of polycrystalline rings in place of discrete spots indicating that the crystal after heating has turned into a polycrystalline material. This

change can be attributed to the oxidation of TaS_2 when heated in air. Therefore to avoid the possibility of oxidation of crystal showing initially a 1T- TaS_2 type structure was heated in a vacuum of 10^{-5} torr at 600°C for 1 hr. and allowed to cool to room temperature. Its a-axis oscillation photograph was then taken (Fig. 8.4). It is seen that this pattern shows no arcing or streaking but in addition to the spots corresponding to 1T-phase faint spots corresponding to 2H-phase also become visible.

It will be observed in the electron microscopic studies of 1T- TaS_2 single crystals described in Chapter 14, that heating a crystal of primarily 1T-phase at room temperature, to higher temperature transforms it to a 2H-phase and upon cooling the specimen from higher temperature to room temperature, the reversible transformation $2\text{H} \rightarrow 1\text{T}$ is seen to occur quite readily.

In the present X-ray diffraction studies heating the crystal from room temperature to 600°C should also bring about the phase transformation (1T \rightarrow 2H) reported above and one should have at higher temperature the presence of 2H-phase in the

oscillation photograph taken at the higher temperature. Since facilities for taking oscillation photograph at higher temperatures were not available photograph shown in Fig. 8.4 was taken after cooling the specimen from 600° C to room temperature. As a result the presence of only discrete 2H-spots could not be detected. Upon cooling the specimen from 600° C to room temperature the reversible transformation from 2H \rightarrow 1T phase takes place. However, certain parts of the crystal can still possess a 2H-phase and so a mixture of 1T and 2H - phases should be seen in the oscillation photograph taken at room temperature. That this is indeed true can be seen in Fig. 8.4, which shows the co-existence of spots corresponding to 1T and 2H phases. The weak intensity of the spots corresponds to 2H phase, indicates that portions containing 2H phase are very small as compared to the portions containing the 1T phase.

A close examination of some of the photographs reveals some sort of arcing, i.e. the diffraction spots are slightly elongated in a direction perpendicular to the layer lines. An example showing pronounced arcing is illustrated in Fig. 8.5. This type of arcing may be because of the interaction

between edge dislocations which render them vertically aligned at a constant spacing²⁾.

The density of dislocations can be estimated by arc length in zero layer line using the following formula¹²⁾,

$$\rho = \frac{\theta}{b}$$

where θ is the angle of tilt and
 b is the Burgers vector.

θ can be calculated by using the following relation for IT-type.

$$\theta = \frac{c}{\lambda} \cdot \frac{n}{l} \cdot \frac{c}{l \cdot r}$$

where c = lattice parameter, c.
 λ = wavelength of X-rays
 n = number of polytypes
 c = arc length and
 r = the camera radius.

Arc length c for (006) reflection in the
 Fig. 8.5 = 0.3 cm.

Thus using all the known values, the

angle of tilt obtained from Fig. 8.5 comes out to be 3.672° , which yields the density of dislocations,
 $= 1.869 \times 10^6 \text{ cm}^{-1}$.

8.6 Conclusions

1. Determination of 'a' and 'c' parameters from X-ray oscillation photographs confirm the crystals to be 1T-TaS₂ type.
2. Crystals are found to undergo phase transformation upon heating them to higher temperature. The co-existence of 1T and 2H phases in such crystals is readily detected when they are cooled to room temperature.
3. The dislocation density as estimated from the oscillation photograph is found to be $1.869 \times 10^6 \text{ cm}^{-1}$. This is fairly in good agreement with the value obtained from the etching method.

8.6 References

1. Verma, A. R. and Krishna, P.
"Polymorphism and Polytypism in Crystals"
John Wiley and Sons, Inc. New York, London,
1966.
2. Trigunayat, G. C. and Verma, A. R.
"Polytypism and stacking faults in crystals
with layer structures" F. Levy (Ed.)
"Crystallography and Crystal Chemistry
of materials with layered structures"
Riedel Publishing Co. London (1976),
269-340.
3. Biltz, W. and Koehler, A.
Z. anorg. all. Chem. 238 (1958) 81.
4. Hagg, G. and Schonberg, N.
Arkiv Kemi. 7 (1962) 9.
5. Jellinek, F.
J. Less Com. Metals 4 (1962) 9.
6. Di Salvo, F. J., Bagly, B. G., Voorheve,
J. M. and Waszczak, J. V.
J. Phys. Chem. Sol. 34 (1973) 1357.
7. Brouwer, R. and Jellinek, F.
Mat. Res. Bull. 9 (1974) 827.
8. Trigunayat, G. C.
Bull. Nat. Inst. Sci. India 14 (1959) 109.
9. Mitchell, R. S.
Z. Krist. 108 (1956) 337.
10. Gulazarilal and Trigunayat, G. C.
J. Cryst. Growth 11 (1971) 177.

11. Gulzarilal and Trigunayat, G. C.
Acta Cryst. A 26 (1970) 430.
12. Agarwal, V. K. and Trigunayat, G. C.
Acta Cryst. A 25 (1969) 401.

Captions of the figures

- Fig. 8.1 The $b^* - c^*$ reciprocal lattice net
for hexagonal TaS_2 polytypes.
- Fig. 8.2 a-axis oscillation photograph
($25 \sim 40^\circ$) for TaS_2 crystals.
- Fig. 8.3 a-axis oscillation photograph
($25 \sim 40^\circ$) of the crystal after
heating at $600^\circ C$ in atmosphere.
- Fig. 8.4 a-axis oscillation photograph
($25 \sim 40^\circ$) of a crystal after
heating a crystal at $600^\circ C$
at 10^{-5} torr.
- Fig. 8.5 a-axis oscillation photograph
($25 \sim 40^\circ$) showing arcing of the
diffraction spots.

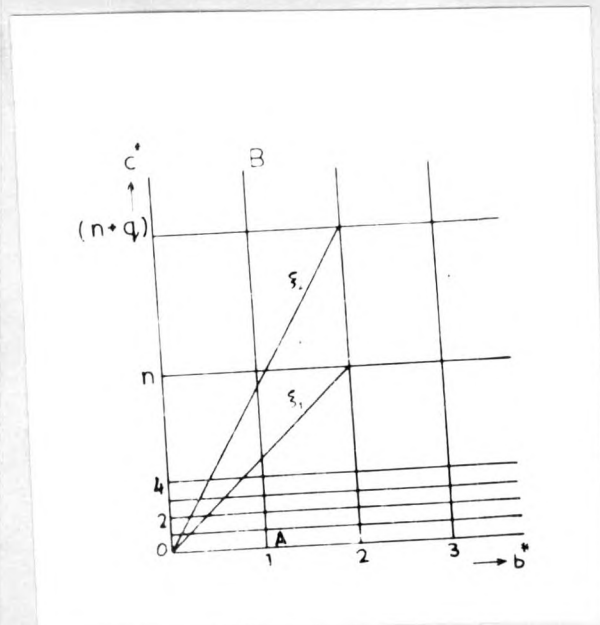


Fig. 8.1

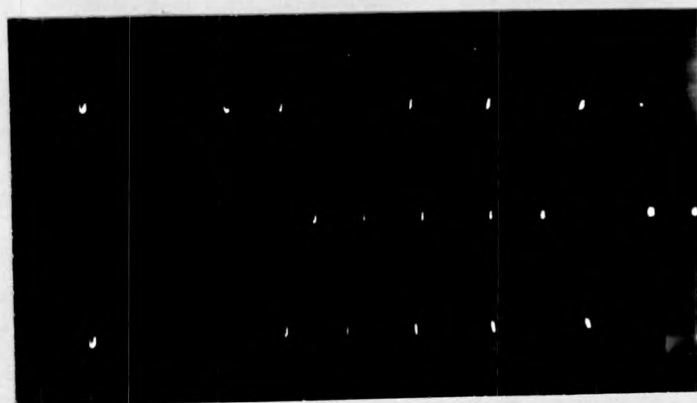


Fig. 8.2

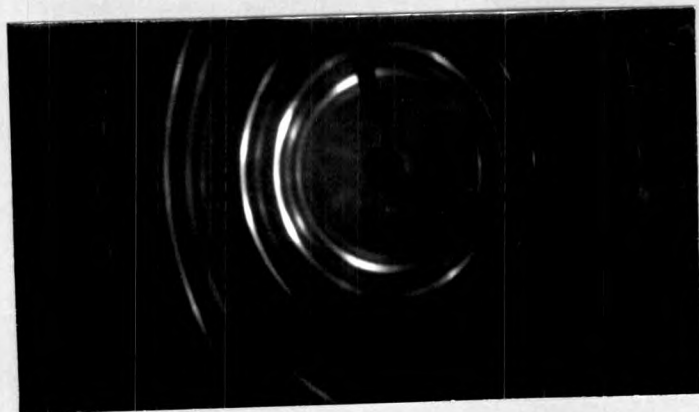


Fig. 8.3

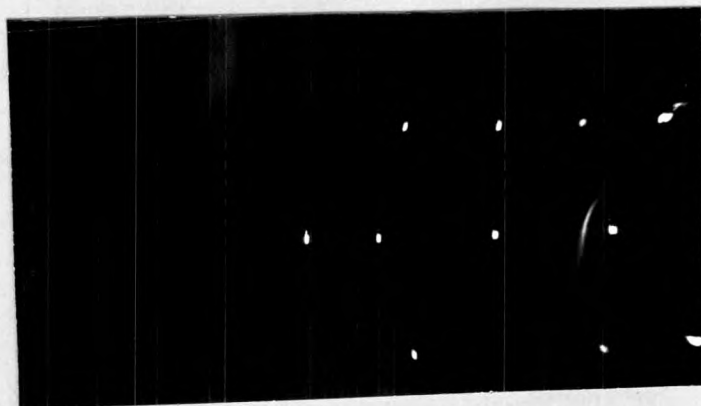


Fig. 8.4

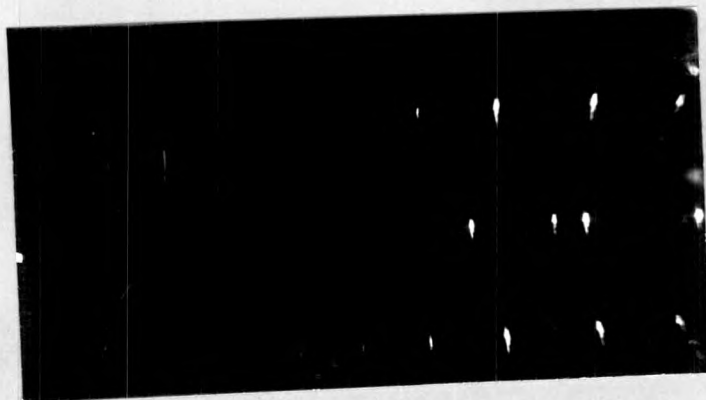


Fig. 8.5